Image-based Quality Assessment of Middle Cerebral Artery Occlusion using SIFT Descriptor and Support Vector Machine

Wuxian He[1*], BSc; Hongtu Tang[2*], PhD; Jia Li[2*], PhD; Chenze Hou[1], Msc; Xiaoyan Shen[3], PhD; Chenrui Li[1], BEng; Huafeng Liu[4], PhD; Weichuan Yu[1], PhD

[1]*Department of Electronic and Computer Engineering, The Hong Kong University of Science and Technology, Hong Kong, China*
[2]*Department of Acupuncture and Moxibustion, Hubei University of Chinese Medicine, Wuhan, China*
[3]*College of Science, Zhejiang University of Technology, Hangzhou, China*
[4]*Department of Optical Engineering, Zhejiang University, Hangzhou, China*

*Contributed equally.

Correspondence to:
Huafeng Liu, PhD, Department of Optical Engineering, Zhejiang University, Hangzhou, China. Email: liuhf@zju.edu.cn. Phone: (+86)571-87951674
Weichuan Yu, PhD, Department of Electronic and Computer Engineering, The Hong Kong University of Science and Technology, Clear Water Bay, Kowloon, Hong Kong, China. Email eeyu@ust.hk. Phone (+852) 23587054
Total number of tables and figures: 3 tables , 2 figures .
Word count: 4890
Short title: MCAO Assessment

Abstract:

Background and Purpose: Quality assessment of middle cerebral artery occlusion (MCAO) is of vital importance to a wide range of animal studies of stroke such as reperfusion therapy. However, a non-invasive and objective assessment method is still lacking. Herein, we propose an image feature-based protocol to assess the quality of the procedure.

Methods: We performed permanent MCAO to a total of 161 Sprague-Dawley rats. Micro positron emission tomography (PET) images were acquired both before and after the MCAO procedure. Triphenyl tetrazolium chloride (TTC) staining was also conducted as a ground truth to ensure the MCAO quality. After preprocessing of the PET images, a combination of 3D scale invariant feature transform (SIFT) and support vector machine (SVM) was applied to extract features and train a classifier that can assess the quality of the MCAO procedure.

Results: 106 rats and 212 images were used as training data to construct the classification model. The SVM classifier achieved over 98% accuracy in cross validation. 10 rats with TTC results served as validation data as the staining showed clear infarction in the ipsilateral brain. Their images were tested by the classifier and all of them were categorized into the correct group. Finally, the remaining 45 rats from a separate experiment were treated as independent test data. The prediction accuracy for their 90 images reached the level of 91%. An online interface was constructed for users to upload their scans and obtain the assessment results.

Conclusion: This image-based protocol provides a convenient, quantitative and non-invasive tool to assess the quality of the MCAO procedure.

Abbreviations and Acronyms:
MCAO: middle cerebral artery occlusion
PET: positron emission tomography
TTC: triphenyl tetrazolium chloride
FDG: fluorodeoxyglucose
CBF: cerebral blood flow
VBM: voxel-based morphometry
SUV: standardized uptake value
SIFT: scale invariant feature transform
SVM: support vector machine
SPM: statistical parametric mapping
PCA: principal component analysis
DoG: difference of Gaussian

Key words: middle cerebral artery occlusion, positron emission tomography, image feature, stroke

Introduction:

Stroke is one of the most serious brain diseases and the second leading cause of death around the world.[1] Animal subjects have been extensively used to study stroke and treatment effects. Among animal subjects, rats are quite popular because of their low cost and similar physiology to humans. To induce focal cerebral ischemia in rat subjects, middle cerebral artery occlusion (MCAO) is the most commonly used procedure.[2] After the occlusion, neurological deficit examinations need to be performed to ensure the success of the MCAO before follow-up experiments can be carried out. Traditionally, behavior tests,[3] and triphenyl tetrazolium chloride (TTC) staining,[4] were used to assess the MCAO quality. However, the behavior test is subjective, and the judgments vary among different examiners.[5] Although TTC staining can provide the ground truth of the MCAO quality, it needs to sacrifice rats. Consequently, follow-up experiments become infeasible.

In recent years, image-based analysis methods using magnetic resonance imaging (MRI), functional MRI (fMRI) or positron emission tomography (PET) have gained popularity due to their objective and non-invasive nature.[6,7] MRI can reveal the anatomical structure of brain but is not capable of measuring metabolic changes during stroke. fMRI measures the blood-oxygen-level dependent (BOLD) signal, which is associated with the brain metabolism. However, it is quite sensitive to movements. Consequently, the head motion of rats during the scan session may generate undesired blurring effect.[8,9] PET is more robust to spatial movements, but suffers from poor resolution. In this study, we adopted microPET to acquire image data. The ^{18}F- fluorodeoxyglucose (FDG) PET is commonly used to provide *in vivo* information of cerebral metabolism. Since the concentration of FDG reveals the cerebral blood flow, existing stroke studies assess the MCAO quality by measuring a reduction of FDG in the ipsilateral hemisphere.[10,11] However, bias and errors could arise due to various factors such as variations of FDG concentration, scanning time and basal metabolic rate.[12] Hence, a fast, accurate and reliable approach to assessing the MCAO quality is desirable.

Here, we adopt a 3D SIFT algorithm[13] to extract features from the FDG-PET images. Then, an SVM classification model is built from the features of labeled images, which can classify an unknown new image into either the healthy or MCAO category with high accuracy. Existing approaches relying on FDG-PET analysis require two scans per subject: one baseline and one taken after MCAO.[11,14] In practice, preparing the radiotracer and taking PET images are expensive and time consuming, especially when a large number of rats are involved in the experiment. Our protocol overcomes such a defect by learning from the data that consists of both baseline and MCAO images. The feature-based property also avoids potential errors introduced during the intensity normalization process.

In the following sections, we shall describe how to perform the image-based assessment, from preprocessing, through feature extraction, to model construction, and demonstrate the significance of the protocol.

Methods:

Animals: All the animal experiments in this study were approved by the Animal Research Committee of School of Medicine, Zhejiang University. Two independent MCAO surgeries were performed following the same procedure,[2] one with 116 rats and the other with 45 rats. The subjects involved in this study were adult female Sprague-Dawley rats with a weight of 180-280 g. During the experiment, each rat had free access to food and water, and was anesthetized using 400 mg/kg chloral hydrate before the scanning. The entire experimental procedure followed the guidelines for the care and use of Laboratory Animals published by the National Institute of Health. All the data are available from the website: http://yulab.ust.hk/MCAO/

Image data acquisition: All 3D FDG-microPET images were acquired with a microPET R4 system (CTI Concorde Microsystems, LLC.) located at the Medical PET Center of Zhejiang University. For each rat in this study, one scan was taken for the resting state (baseline) before the MCAO procedure and one was taken after the MCAO procedure. Both scans were acquired after 30 minutes of ^{18}F-FDG injection and each lasted for 15 minutes. The spatial resolution of the scanner was 1.9 mm full width at half maximum (FWHM) in the transverse plane and 1.88 mm FWHM in the axial plane. Additionally, 10 rats from the first experimental group were chosen randomly to have TTC staining. The results provided clear visualization of the tissue damage in the right brain, and photos were taken as a record for validation.

FDG-PET template: To transform PET scans of distinct rats into a standard space, a template was necessary. Since there is no widely accepted PET template for Sprague-Dawley rats, we constructed our own template from an existing MRI template[15] using SPM12 (Wellcome Department of Cognitive Neurology, London, UK). The detailed steps are described in the Online Data Supplement. The MRI template we used and the PET template we constructed are shown in Figure 1A.

Preprocessing: The raw data were reconstructed using the maximum a posterior (MAP) algorithm.[16] Then, scans were preprocessed with the constructed template in SPM12. The pipeline of the preprocessing is shown in the Online Data Supplement. Figure 1B shows an example of a raw image and its preprocessed result.

Image features: After spatial preprocessing, image features were extracted using the 3D SIFT method. The Original SIFT is used for 2D images[17] and the detailed algorithm can be found in the Online Data Supplement. Since the PET images were three dimensional, we adopted a 3D SIFT algorithm to extract features, and the length of the final descriptor was a vector in 768 dimensions.[13] Since the images had already been registered, we used a set of fixed key points and omitted the key point localization step. Furthermore, because SIFT extracts local features from an image, we proposed to choose key points from brain areas that are possibly affected during a stroke, such as the neocortex or striatum.[18] The delineation of brain regions (one slice is shown in Figure 1C) was based on the Waxholm atlas made by Papp et al.[19] Because the symptoms and injured areas resulting from a stroke are not totally understood, in order to be inclusive, after many trials we determined 25 key points from 13 brain regions, as shown in Table 1. Then the feature of each image was formed by concatenating the descriptors of all the

25 key points of it, which became a vector in 768*25=19200 dimensions. In the Online Data Supplement, we provide a figure showing the 3D rendered atlas along with the location of the 25 key points. The 3D rendering was completed by using an open-source data visualization application called ParaView.[20]

Statistics and model building: The calculations and statistical analysis were done in MATLAB R2018b (Natick, Massachusetts: The MathWorks Inc). The image features of all the training data were used to learn a linear SVM classification model. This model can be used to classify any new image into one of the two groups: normal (baseline) or MCAO (injured). The assessment of MCAO quality is based on the classification or prediction accuracy. Ten-fold cross validation was used to examine the performance of the model, and classification on the validation set and test set was also conducted to evaluate the performance.

Results:

Key points and features: The brain regions from which we chose key points, along with the number of key points in each of them, are shown in Table 1. The neocortex was the largest region and contained voxels in a wide range. Thus, we chose the largest number of key points from it. Meanwhile, the striatum was the second largest region, and therefore we chose 3 key points from it. The decision to use these brain regions and key points was based on existing stroke studies[18,21] and on our repeated experiments with different sets of key points.
The feature of each PET image was obtained by concatenating the 25 SIFT descriptors into a single vector. As mentioned previously, we have 106 rats in the training set, 10 rats (with TTC ground truth) in the validation set and 45 rats (from an independent experiment) in the test set. Every rat was given two PET scans, one before the MCAO surgery, which we call the normal image, and one after the surgery, which we call the MCAO image. Prior to training the SVM classification model, we performed principal component analysis (PCA) to the image features. As an unsupervised learning method, PCA can significantly reduce the feature dimensionality by projecting the data onto its principal vectors. This enables us to project the image features from a 19200-dimensional space to a 2-dimensional plane and visualize them. Figure 2A shows the PCA results of the two sets of image features, and both of them indicate a clear discrimination between normal and MCAO images. This label-free result suggests that the use of SIFT descriptors has promising accuracy to assess MCAO quality.

Prediction accuracy: Although PCA returned significant results, its computation requires grouped data. Therefore, it cannot be applied to a single test image. For this reason, we turned to use supervised classification approaches. In order to make our protocol as simple as possible, we used basic and well-known classification methods. We chose the following traditional methods: K-nearest neighbor (KNN), decision tree, linear discriminant analysis (LDA) and support vector machine (SVM) and tested their accuracy with cross validation.[22] The results shown in Figure 2B suggest that SVM is the optimal method with the highest accuracy. The classification accuracy with cross validation reached over 98% and the prediction accuracy for the test set was 91%. SVM was therefore adopted for the protocol.

Validation with biomedical indicator: All the analyses so far treated the rats after MCAO as if their surgery were completed successfully. Although the MCAO procedures were carried out carefully, the results became less convincing if the ground truth of occlusion could not be validated through a direct measure. Therefore, we performed TTC staining on 10 randomly selected rats and the results all showed obvious brain infarction in the right half of the brain (one example is shown in Figure 1D). We then tested the 20 images (10 normal + 10 MCAO) with the SVM model trained from the 106 rats, and obtained 100% accuracy. All the TTC staining photos of the 10 rats are shown on our webpage.

Discussion:

Comparison with state-of-the-art methods: Our study was conducted using a large number of rats with PET images acquired before and after MCAO. The size of our dataset was larger than that in most of the existing MCAO studies, and therefore we could investigate various methods and obtain reliable results for the assessment. Our protocol can also be applied to assess the MCAO quality using only a single image, and does not require the scan of the normal state before occlusion. This is a significant advantage over the current image-based assessment approaches. The existing intensity-based methods all require two scans of the subject: one baseline image and one after MCAO, and significant findings can be made only when a clear intensity change between the two images is observed in an injured area.[10,11,23]

Moreover, we found that signal changes among different rats were not consistent after we performed one popular intensity-based method called the voxel-based morphometry (VBM)[24]. The VBM approach was based on the voxel-wise or region-wise comparison between the signal change of the radiotracer concentration. In the FDG-PET study of the MCAO procedure, the intensities will directly indicate the uptake of glucose, and assessment of the MCAO is feasible if a significant intensity decrease is observed. However, the intensity value of a PET scan is directly related to the radiotracer concentration. Because the concentration cannot be maintained at the same level for each injection, the intensity needs to be normalized by the average intensity value among all the intracerebral voxels for each rat.[25] Such intensity normalization steps produce the standardized uptake value (SUV), and the SUV change in two injured regions before and after MCAO from our dataset is shown in Figure 2C.

Figure 2C shows that the SUV change on two significant regions has non-uniform results. About one quarter of the total rats had increased FDG intake after MCAO even though we performed intensity normalization. As discussed previously, this phenomenon is due to the drawback of intensity normalization. This is because the mean intensity in the intracranial part is largely determined by the healthy regions since the injured area will have negligible FDG uptake. If two rats have significantly different amounts of FDG injected, the overall intensity in the whole brain will vary significantly, and thus the denominator becomes a dominating factor.[26] In this way, the normalized intensity in the injured brain may even increase after MCAO if less FDG is injected before the scanning session. Using our feature-based protocol, we could overcome this problem and bring higher accuracy (Table 2). At the same time, taking only one scan per rat could save time and cost associated with PET scanning in these

experiments.

Robustness of the PET template: We provided a ready-to-use PET template of Sprague-Dawley rats for raw image preprocessing. This template could be useful to researchers who desire a PET template but lack data to construct one themselves. To ensure the 20 baseline images for the construction were able to build a representative and universal template, we studied multiple choices of the baseline images and verified the template quality. Since we had two independent datasets, we tested 7 different combinations of images:

(1) 20 baseline images with good initial alignments carefully chosen from the training set.
(2) 20 baseline images randomly chosen from the training set.
(3) 10 baseline images randomly chosen from the training set and 10 baseline images from the test set.
(4) 20 baseline images randomly chosen from the test set.
(5) 20 baseline images with a high intensity level (12.92~17.44) from the training set.
(6) 20 baseline images with a low intensity level (1.848~2.786) from the training set.
(7) 10 baseline images with a high intensity level and 10 with a low intensity level from the training set.

We examined the quality of the constructed templates based on SVM accuracy. The results shown in Table 3 indicate that the choice of baseline images had a minor influence on the template quality and preprocessing steps. Even when we selected the baseline images only from one dataset and performed preprocessing and analysis on the other dataset, the result showed very good consistency. Therefore, the final template we fixed was the one from (1) above using 20 optimal baseline images from the training set.

SIFT and feature pattern: The conventional SIFT algorithm locates key points by looking for the space extrema through the Difference of Gaussian (DoG). We tried to extract the space extrema for the 3D images in a four-dimensional neighborhood with the DoG. Only a few key points were returned from the calculation, while some images had no extrema. This was due to the nature of the PET images, where neighboring voxels were highly correlated because of the continuous FDG concentration in the brain and the smoothing step in the preprocessing.[27] Thus, for our 3D PET images, which were registered to the template, we decided to use a fixed set of key points which are all in the regions that are shown in previous studies to be affected by the MCAO procedure. In this way, the extracted descriptors from different images had the same locations and thus could be compared among each other.

After concatenating the SIFT descriptors of 25 key points into one feature vector, we performed dimensionality reduction through PCA and obtained significant results. The two plots in Figure 2A both show a trend that the blue data points (normal images) tend to be clustered, whereas the orange points (MCAO images) have a larger variance. This phenomenon suggests that the MCAO surgery will have different influence on different rats due to individual differences or distinct trials.[28] The discrepancy of the infarction severity may lead to incorrect statistical decisions if we adopt the voxel-based morphometry. By using the SVM model, we clearly show that such a discrepancy is still much smaller than the difference between normal images and MCAO images and can therefore be reliably treated as intra-class variation.

Tool availability and online interface: All the data and tools included in this paper are available for open access on the webpage: http://yulab.ust.hk/MCAO/. Furthermore, to facilitate the application of our method, we constructed an online interface that can automatically perform the image preprocessing, feature extraction and MCAO assessment. Users only need to do one manual step that roughly align their images to one example we provided before they upload. This is to ensure the accuracy of preprocessing results because we assume that different PET scans will have varying resolution and orientations.

Limitations: Our study still has room for improvement. For example, there were thousands of voxels in the injured areas, so it was infeasible to check each of them one by one and find an optimal key point. We expect that researchers who are expert in knowing exactly where the brain ischemia and infarctions happen can provide more accurate key point locations. Additionally, the study of using other image features apart from SIFT is an interesting topic and an open problem.

Conclusion:

This paper presented a protocol to assess the quality of rat MCAO procedure by extracting SIFT features and building an SVM model from the PET imaging data. It has advantages over behavior tests or TTC staining by providing quantitative and non-invasive measurements. Unlike existing image-based methods (such as the VBM) that suffer from potential bias caused by uncontrollable FDG dosage difference, our protocol can provide reliable classification results without intensity normalization. Moreover, our method does not rely on comparison between scans before and after the MCAO, and therefore the baseline scan is not always required when designing the experiment. This will be beneficial when the proposed experiment involves large number of subjects.

Acknowledgments: We thank Jingwen Zheng for kindly helping setting up the webpage and Tamie KONSTAS for carefully proofreading the manuscript.
Sources of Funding: This work was supported in part by the National Natural Science Foundation of China (No: 61525106, U1809204), the National Key Technology Research and Development Program of China (No: 2017YFE0104000) and R4012-18 from the Research Grant Council (RGC) of the Hong Kong S.A.R. government of China.
Disclosures: None.

References:

1. Johnson W, Onuma O, Owolabi M, Sachdev S. Stroke: a global response is needed. *Bulletin of the World Health Organization*. 2016;94:634.
2. Longa EZ, Weinstein PR, Carlson S, Cummins R. Reversible middle cerebral artery occlusion without craniectomy in rats. *Stroke*. 1989;20:84-91.
3. Bederson JB, Pitts LH, Tsuji M, Nishimura MC, Davis RL, Bartkowski H. Rat middle cerebral artery occlusion: evaluation of the model and development of a neurologic examination. *Stroke*. 1986;17:472-476.

4. Benedek A, Móricz K, Jurányi Z, Gigler G, Lévay G, Hársing Jr LG, Mátyus P, Szénási G, Albert M. Use of TTC staining for the evaluation of tissue injury in the early phases of reperfusion after focal cerebral ischemia in rats. *Brain research*. 2006;1116:159-165.
5. Bieber M, Gronewold J, Scharf AC, Schuhmann MK, Langhauser F, Hopp S, Mencl S, Guess E, Leinweber J, Guthmann J, et al. Validity and Reliability of Neurological Scores in Mice Exposed to Middle Cerebral Artery Occlusion. *Stroke*. 2019;50:2875-2882.
6. Kreisl WC, Kim MJ, Coughlin JM, Henter ID, Owen DR, Innis RB. PET imaging of neuroinflammation in neurological disorders. *The Lancet Neurology*. 2020;19:940-950.
7. Nael K, Khan R, Choudhary G, Meshksar A, Villablanca P, Tay J, Drake K, Coull BM, Kidwell CS. Six-minute magnetic resonance imaging protocol for evaluation of acute ischemic stroke: pushing the boundaries. *Stroke*. 2014;45:1985-1991.
8. Friston KJ, Williams S, Howard R, Frackowiak RS, Turner R. Movement-related effects in fMRI time-series. *Magnetic Resonance in Medicine*. 1996;35:346-355.
9. Power JD, Mitra A, Laumann TO, Snyder AZ, Schlaggar BL, Petersen SE. Methods to detect, characterize, and remove motion artifact in resting state fMRI. *Neuroimage*. 2014;84:320-341.
10. Worsley KJ, Evans AC, Marrett S, Neelin P. A three-dimensional statistical analysis for CBF activation studies in human brain. *Journal of Cerebral Blood Flow & Metabolism*. 1992;12:900-918.
11. Li Y, Zhang B, Yu K, Li C, Xie H, Bao W, Kong Y, Jiao F, Guan Y, Bai Y. Effects of constraint-induced movement therapy on brain glucose metabolism in a rat model of cerebral ischemia: a micro PET/CT study. *International Journal of Neuroscience*. 2018;128:736-745.
12. Nie B, Liang S, Jiang X, Duan S, Huang Q, Zhang T, Li P, Liu H, Shan, B. An automatic method for generating an unbiased intensity normalizing factor in positron emission tomography image analysis after stroke. *Neuroscience bulletin*. 2018;34:833-841.
13. Rister B, Reiter D, Zhang H, Volz D, Horowitz M, Gabr RE, Cavallaro JR. Scale-and orientation-invariant keypoints in higher-dimensional data. Paper presented at: *2015 IEEE International Conference on Image Processing (ICIP)*; September 27-30, 2015; Quebec City, Canada. (pp. 3490-3494). IEEE. https://ieeexplore.ieee.org/abstract/document/7351453. Accessed November 9, 2020.
14. Walberer M, Backes H, Rueger MA, Neumaier B, Endepols H, Hoehn M, Fink GR, Schroeter M, Graf R. Potential of early [18F]-2-fluoro-2-deoxy-D-glucose positron emission tomography for identifying hypoperfusion and predicting fate of tissue in a rat embolic stroke model. *Stroke*. 2012;43:193-198.
15. Schweinhardt P, Fransson P, Olson L, Spenger C, Andersson J L. A template for spatial normalisation of MR images of the rat brain. *Journal of Neuroscience Methods*. 2003;129:105-113.
16. Levitan E, Herman GT. A maximum a posteriori probability expectation maximization algorithm for image reconstruction in emission tomography. *IEEE Transactions on Medical Imaging*. 1987;6:185-192.
17. Lowe DG. Distinctive image features from scale-invariant keypoints. *International Journal of Computer Vision*. 2004;60:91-110.
18. Popp A, Jaenisch N, Witte OW, Frahm C. Identification of ischemic regions in a rat model of stroke. *PloS one*. 2009;4:e4764.
19. Papp EA, Leergaard TB, Calabrese E, Johnson GA, Bjaalie JG. Waxholm Space atlas of the Sprague Dawley rat brain. *Neuroimage*. 2014;97:374-386.
20. Ahrens J, Geveci B, Law C. Paraview: An end-user tool for large data visualization. The Visualization Handbook. Elsevier; 2005.
21. Butler TL, Kassed CA, Sanberg PR, Willing AE, Pennypacker KR. Neurodegeneration in the rat hippocampus and striatum after middle cerebral artery occlusion. *Brain Research*. 2002;929:252-260.

22. Hastie T, Tibshirani R, Friedman J. The elements of statistical learning: data mining, inference, and prediction. Springer Science & Business Media; 2009.
23. Worsley KJ, Marrett S, Neelin P, Vandal AC, Friston KJ, Evans AC. A unified statistical approach for determining significant signals in images of cerebral activation. *Human Brain Mapping*. 1996;4:58-73.
24. Ashburner J, Friston KJ. Voxel-based morphometry—the methods. *Neuroimage*. 2000;11:805-821.
25. López-González FJ, Silva-Rodríguez J, Paredes-Pacheco J, Niñerola-Baizán A, Efthimiou N, Martín-Martín C, Moscoso A, Ruibal Á, Roé-Vellvé N, Aguiar P. Intensity normalization methods in brain FDG-PET quantification. *NeuroImage*, 2020;222:117229.
26. Ashburner J, Friston KJ, Penny W. Human brain function, in chapter: The general linear model. Academic press; 2004.
27. Arnberg F, Grafström J, Lundberg J, Nikkhou-Aski S, Little P, Damberg P, Mitsios N, Mulder J, Lu L, Söderman M, et al. Imaging of a clinically relevant stroke model: glucose hypermetabolism revisited. *Stroke*. 2015;46:835-842.
28. Leithner C, Füchtemeier M, Jorks D, Mueller S, Dirnagl U, Royl G. Infarct volume prediction by early magnetic resonance imaging in a murine stroke model depends on ischemia duration and time of imaging. *Stroke*. 2015;46:3249-3259.

Figure legends:

Figure 1. Experimental procedures. **A**: The existing MRI template (left) and the FDG-PET template (right) that we constructed. **B**: One example of the raw scan after reconstruction (left) and the corresponding brain image after preprocessing (right). **C**: An example of the TTC staining result after 15 hours of occlusion. **D**: A coronal slice of the Waxholm atlas showing brain region delineation.

Figure 2. Results from statistical analysis of the image features and histograms from VBM. **A**: The PCA results of the two sets of image features. Features in the original 19200-dimensional space were projected to a 2-dimension plane. Left: data from the training set; Right: data from the test set. **B**: Box plot and scatter plot of accuracy for different classification methods. The box plot represents the 10-fold cross validation accuracy with different classification methods using the 106 rats from the training set. The orange scatter points were obtained from predicting the 45 rats in the independent test set using each trained model. **C**: Histograms of the SUV (normalized intensity) change between the normal and MCAO images (MCAO - normal) for all rats in the training set from two regions: the striatum (left) and the neocortex (right). Orange bins represent the subjects with increased SUV in the ipsilateral part after MCAO.

Tables:

Table 1. The brain regions from which the 25 key points were chosen. Regions with more voxels and severe damage, such as neocortex and striatum, have multiple key points. The regions are listed in the same order according to the region index provided in the Waxholm Space atlas.

Region name	Number of key points
subthalamic nucleus	1
alveus of the hippocampus	1
striatum	3
ventral hippocampal commissure	1
thalamus	2
fimbria of the hippocampus	1
stria medullaris of the thalamus	1
interpeduncular nucleus	1
middle cerebellar peduncle	1
neocortex	10
postrhinal cortex	1
perirhinal area 35	1
perirhinal area 36	1
Total number:	25

Table 2. Comparison of results between using VBM and our proposed classification method. VBM was performed in 4 regions of interest: striatum, thalamus, fimbria of the hippocampus and neocortex from the training dataset. The number of rats that showed significant intensity decrease ($p<0.05$, one-sided *t*-test) were counted and divided by the total number. The ratio was compared with the classification accuracy using our feature-based method.

Method	Region/Point	Number of subjects		Ratio/accuracy
		Significant decrease	Total	
Voxel-based morphometry	Striatum	89	106	83.96%
	Thalamus	80	106	75.47%
	Fimbria of the hippocampus	90	106	84.91%
	Neocortex	84	106	79.25%
Proposed method	25 key points	-	106	97.41%

Table 3. Seven distinct combinations of baseline images chosen to construct the PET template. For each experiment, all images were preprocessed using the constructed template followed by SIFT feature classification, and the accuracy with cross validation was recorded as a measure of the template quality.

Number of baseline images		Classification accuracy	
Training set	Test set	Training set	Test set
20 in good initial alignment	0	99.14%	97.76%
20 chosen randomly	0	98.86%	92.71%
10 chosen randomly	10 chosen randomly	98.71%	94.03%
0	20 chosen randomly	98.50%	93.30%
20 in high intensity level	0	98.73%	93.37%
20 in low intensity level	0	98.19%	92.90%
10 in high + 10 in low intensity level	0	98.62%	92.98%

Figures:

Figure 1

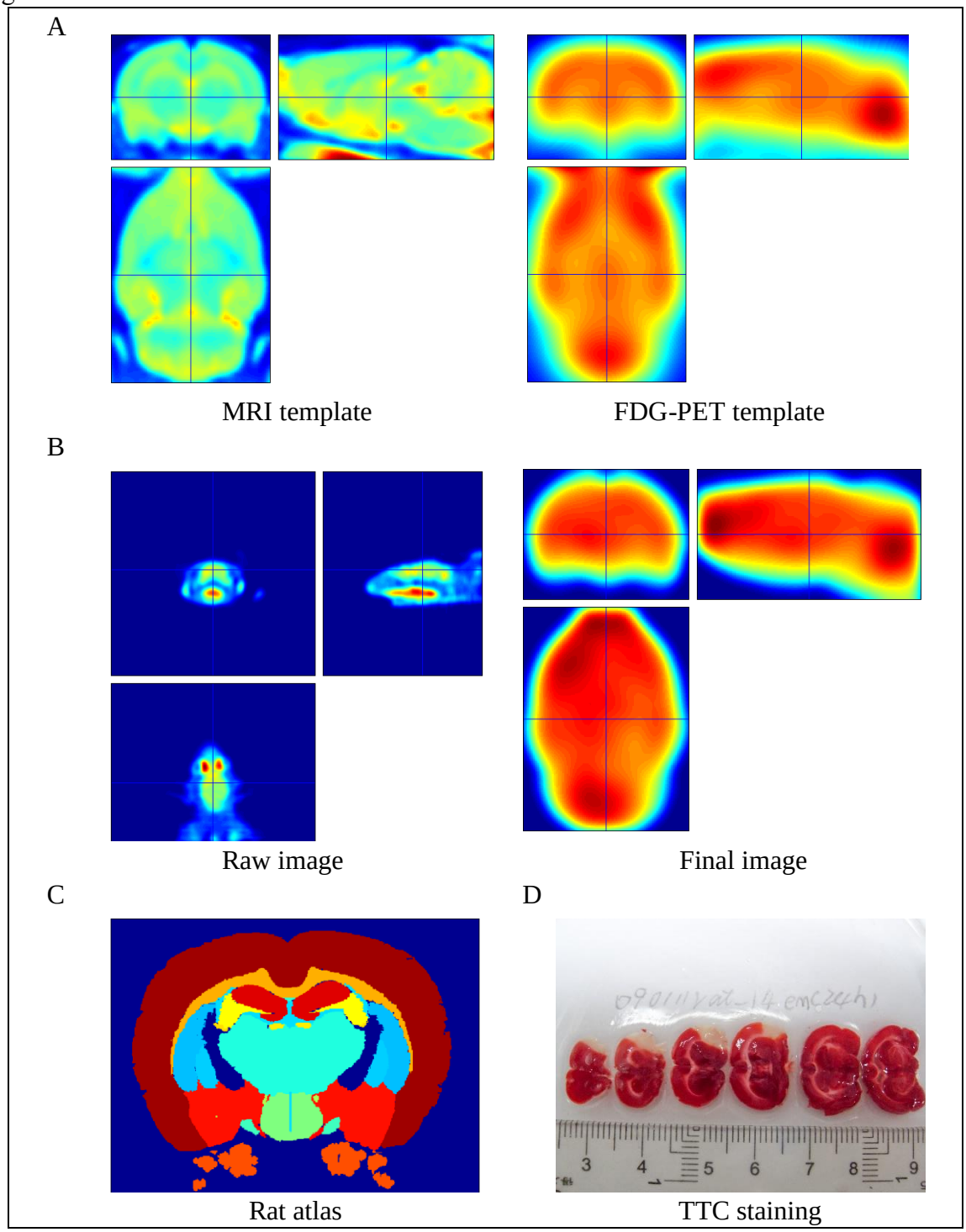

Figure 2

A

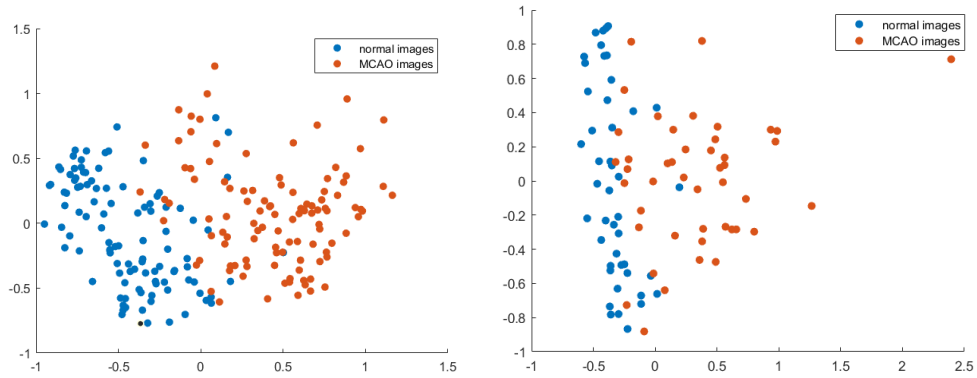

Training dataset Testing dataset

B

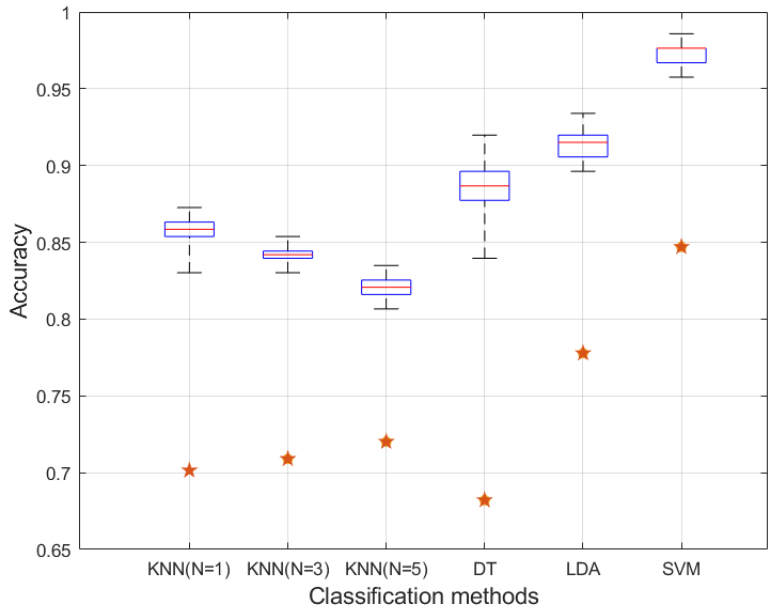

Classification accuracy

C

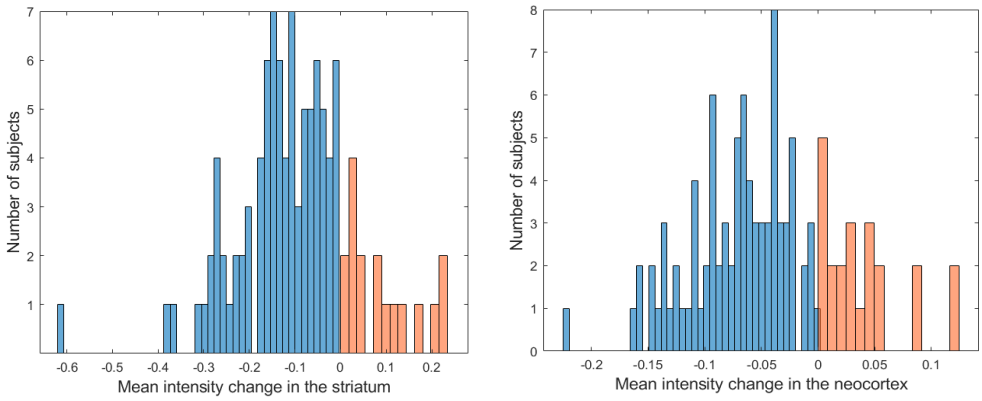

Histograms of mean intensity change in two affected regions